Biogeosciences Discuss., 5, 4161–4207, 2008
www.biogeosciences-discuss.net/5/4161/2008/

Biogeosciences Discussions

Biogeosciences Discussions is the access reviewed discussion forum of *Biogeosciences*

Simulating carbon exchange using a regional atmospheric model coupled to an advanced land-surface model

H. W. Ter Maat and R. W. A. Hutjes

ESS-CC (Earth System Science-Climate Change), Alterra - Wageningen UR, Wageningen, The Netherlands

Received: 28 July 2008 – Accepted: 4 September 2008 – Published: 29 October 2008

Correspondence to: H. W. Ter Maat (herbert.termaat@wur.nl)

Published by Copernicus Publications on behalf of the European Geosciences Union.

Abstract

A large scale mismatch exists between our understanding and quantification of ecosystem atmosphere exchange of carbon dioxide at local scale and continental scales. This paper will focus on the carbon exchange on the regional scale to address the following question: What are the main controlling factors determining atmospheric carbon dioxide content at a regional scale? We use the Regional Atmospheric Modelling System (RAMS), coupled with a land surface scheme simulating carbon, heat and momentum fluxes (SWAPS-C), and including also sub models for urban and marine fluxes, which in principle include the main controlling mechanisms and capture the relevant dynamics of the system. To validate the model, observations are used which were taken during an intensive observational campaign in the central Netherlands in summer 2002. These included flux-site observations, vertical profiles at tall towers and spatial fluxes of various variables taken by aircraft.

The coupled regional model (RAMS-SWAPS-C) generally does a good job in simulating results close to reality. The validation of the model demonstrates that surface fluxes of heat, water and CO_2 are reasonably well simulated. The comparison against aircraft data shows that the regional meteorology is captured by the model. Comparing spatially explicit simulated and observed fluxes we conclude that in general simulated latent heat fluxes are underestimated by the model to the observations which exhibit large standard deviation for all flights. Sensitivity experiments demonstrated the relevance of the urban emissions of carbon dioxide for the carbon balance in this particular region. The same test also show the relation between uncertainties in surface fluxes and those in atmospheric concentrations.

1 Introduction

A large mismatch exists between our understanding and quantification of ecosystem atmosphere exchange of carbon dioxide at local scale and continental scales. By ad-

BGD

5, 4161–4207, 2008

Simulation of carbon exchange using a regional model

H. W. Ter Maat and R. W. A. Hutjes

dressing in this paper some of the complexities emerging at intermediate scales, a contribution is made to close this scale jump.

At the global scale, inverse modelling with atmospheric tracer transport models has been used to obtain the magnitude and distribution of regional CO_2 fluxes from variations in observed atmospheric CO_2 concentrations. However, according to Gurney et al. (2002) no consensus has yet been reached using this method and more recent "progress" in inversion modelling developments paradoxically lead to more divergent estimations. Gerbig et al. (2003) suggests that models require a horizontal resolution smaller than 30 km to resolve spatial variation of atmospheric CO_2 in the boundary layer over the continent.

At the local scale, eddy-flux observation sites throughout the world are trying to estimate the carbon exchange of various ecosystems within reasonable accuracy (Valentini et al., 2000; Janssens et al., 2003). These surface fluxes show a large variability over various vegetated areas. Together with the vertical mixing in the atmosphere, these surface fluxes vary diurnally and seasonally leading to the rectifier effect, which is difficult to capture in large scale transport models (Denning et al., 1995, 1999). Earlier studies (e.g. Bakwin et al., 1995) showed also the importance of processes like fossil fuel emission and biospheric uptake on the amplitude and magnitude of diurnal and seasonal cycles of CO_2 concentration ([CO_2]).

The hypothesis is that the uncertainties mentioned before can be reduced at the regional level when a good link between local and global scale can be established. A critical role at the regional level is played by the planetary boundary layer (PBL) in transporting CO_2 away from the biosperic and anthropogenic sources at the surface. PBL processes which influence the local CO_2 concentration are entrainment of free tropospheric CO_2 (de Arellano et al., 2004), subsidence, lateral advection of air containing CO_2 and convective processes leading to boundary layer growth (Culf et al., 1997). Local and global scales can be linked experimentally by a monitoring campaign of a certain region in spatial and temporal terms (Dolman et al., 2006; Gioli et al., 2004; Betts et al., 1992), preferably combined with model analyses using regional atmospheric transport models of high resolution (Perez-Landa et al., 2007a, 2007b; Sarrat et al., 2007).

This paper will focus on modelling the regional carbon exchange of a certain region so that an attempt can be made to quantify CO_2 fluxes from various sources at the surface. The following question will be addressed: What are the main controlling factors determining atmospheric carbon dioxide concentration at a regional scale?

To study this regional scale interaction it is important to use land surface descriptions of appropriate complexity, which in principle include the main controlling mechanisms and capture the relevant dynamics of the system, and to represent the real-world spatial variability in soils and vegetation. In this study we use a coupled model, basically consisting of the Regional Atmospheric Modelling System (RAMS, Pielke et al., 1992; Cotton et al., 2003) coupled with a land surface scheme carrying carbon, heat and momentum fluxes (SWAPS-C, Soil Water Atmosphere Plant System-Carbon, Ashby, 1999; Hanan et al., 1998; Hanan, 2001). Area of interest is the Netherlands where in 2002 an intensive measurement campaign was held for two weeks, as part of the EU-financed RECAB project ("Regional Assessment and monitoring of the CArbo Balance within Europe"), which provided a large database to calibrate and validate the models.

First, a description of the modelling system will be given, together with the various databases which are incorporated in the atmospheric model and how some databases are disaggregated in time and space. A short description of the measurement campaign will also be provided detailing the various observations taken and a summary of the weather systems observed during the campaign.

Next, the results of the coupled model will be presented and compared against the observations followed by a discussion of these results. This paper will conclude with a discussion of the carbon dioxide content at a regional scale and the factors controlling this.

2 Description of methods/observations

2.1 Modelling system

The forward modelling system used in this study is the RAMS model version 4.3. The model is 3-D, non-hydrostatic, based on fundamental equations of fluid dynamics and includes a terrain following vertical coordinate system. Together with its nesting options these allow it to be used in high resolution modes. In its standard form, the version used does not include CO_2 as a tracer nor any related surface fluxes. Amongst other reasons we therefore coupled RAMS to SWAPS-C, including CO_2 fluxes from assimilation and respiration. The land surface scheme uses the tile-approach for treating sub grid variability in vegetation and soils, in our implementation 4 tiles per grid box (1 water tile and 3 land tiles). The coupling was implemented in such a way that both models retained full functionality (Fig. 1). The standalone version of SWAPS-C allows easy calibration of its parameters on measured flux datasets (Ter Maat et al., 2008). RAMS allows for passive atmospheric transport of any number of scalars and this has been implemented for CO_2.

Surface layer turbulent mixing follows the standard formulation in RAMS and uses identical diffusion parameterisations for all three scalars (temperature, humidity and CO_2). Unlike the other scalars, temperature and water vapour, atmospheric CO_2 fields are not nudged to some pre-determined large scale analysis during long model integrations. Instead a different approach was followed using the interactive nesting routine in RAMS. The smallest domain has been nested in two larger domains and the atmospheric CO_2 fields at the boundary are obtained from the parent grid (see Fig. 2). Thus, CO_2 concentrations are free to develop, after the initial horizontal homogeneous initialisation from (aircraft) observed concentration profiles. We assume that the spatial differences in [CO_2] in the smallest domain, resulting from emissions and/or uptake at the surface, are larger than the spatial differences in background [CO_2] for the smallest domain. Higher [CO_2], as a result of CO_2-emissions originating from cities outside the smallest domain (e.g. London and major cities in the Ruhr Area in Germany), will also

BGD

5, 4161–4207, 2008

be fed back into the smallest domain through the interactive nesting routine. Observations at the observatory in Mace Head at the west coast of Ireland demonstrated the small differences in background [CO_2] in relative clean air masses under northern hemispheric background conditions (Derwent et al., 2002). Since our analysis focuses on the smallest domain we assume that reasonable realistic horizontal gradients and associated advective fluxes develop along its edges, as a result of flux variability at the largest scales. The typical RAMS configuration used in this study is given in Table 1.

RAMS is forced by analysis data from the European Centre for Medium-Range Weather Forecasts (ECMWF) global model. The grid spacing of the forcing data is 0.5 by 0.5 degree and available every 6 h. Monthly sea surface temperatures have been extracted from the Met Office Hadley Centre's sea ice and sea surface temperature (SST) data set, HadISST1 (Rayner et al., 2003).

CO_2 surface fluxes come from either of three sources:

- Terrestrial biospheric fluxes simulated by SWAPS-C.
- Marine biospheric fluxes computed from large scale observed partial CO_2 pressures in the marine surface layer.
- Anthropogenic CO_2 emissions.

Each of these will be described in the following sections.

2.2 Terrestrial biospheric fluxes

The land surface model SWAPS was extended with a carbon assimilation and respiration routine. The strength of SWAPS-C (Ashby, 1999), is that within the model above- and below-ground processes are represented in similar physical details and that in earlier studies it has been shown that the model simulates energy fluxes and long-term soil moisture (Kabat et al., 1997) very well. The model allows for three different canopy architectures with a mean canopy flow regulating interaction of fluxes

BGD

5, 4161–4207, 2008

H. W. Ter Maat and R. W. A. Hutjes

from upper and lower layers (Dolman, 1993). Photosynthesis and respiration are parameterised using the equations used by Collatz et al. (1992), Hanan et al. (1998), and Lloyd et al. (1995). Although these equations were originally developed for leaf scale, they are applied at canopy scale in this study assuming the canopy can be described as a "big leaf". For parameters necessary in the equations, we used both optimized parameters (coniferous forest, grasslands) and parameters taken from literature (e.g. Ogink-Hendriks, 1995; Spieksma et al., 1997; Van Wijk et al., 2000; Soet et al., 2000; Knorr, 2000) for each landuse class (see Table 2). The optimized parameters are found by minimizing the sum of squares of model predictions and measurements using a Marquardt-Levenberg algorithm for optimization (Marquardt, 1963). The robustness of the parameters for various coniferous sites in Europe is more in depth described by Ter Maat et al. (2008).

Landuse classes have been extracted from the PELCOM database (Mücher et al., 2001) with a resolution of 1 km (Fig. 3). Soil properties were derived from the IGBP-DIS Soil Properties database (Global Soil Data Task Group, 2000) which has a resolution of approximately 10 km (Fig. 4). In RAMS overlays are generated using vegetation and soil maps and then for each grid box the most frequently occurring soil-vegetation combination is determined, which are then assigned to the number of sub-grid tiles effective in that particular implementation.

2.3 Marine biospheric fluxes

Another source of CO_2 fluxes is related to the exchange of carbon between ocean and atmosphere. This exchange has been based on the global compilation of the partial pressure of CO_2 (pCO_2) by Takahashi et al. (1997). The reference year of this climatological database is 1990 and its resolution is 5 by 4 degrees on a monthly basis (see Fig. 5). From this seasonally varying partial pressure we derive the CO_2-flux given a certain pCO_2 depending on simulated wind speed and to a lesser degree on sea surface temperature following Wanninkhof (1992) and Weiss (1974). To prevent unrealistic sharp flux jumps at resolutions higher than the original 5 by 4 degrees, we downscaled the dataset to 1×1° by simple linear interpolation.

2.4 Anthropogenic CO_2 emissions

Anthropogenic emissions from, for example, road transport, power generation and air traffic are important CO_2 sources in our domain. The emission inventory implemented in the RAMS/SWAPS-modelling system is the EDGAR 3.2 database (Olivier and Berdowski, 2001). The spatial resolution of this database is 1 by 1 degree and annual emissions of CO_2 are available for 1995 (see Fig. 6). Emissions over the oceans from shipping and upper-air emissions from air traffic were neglected in this process.

To get a better spatial representation of anthropogenic emissions, these emissions are disaggregated in space. This is done by equally distributing the emissions of a particular 1×1° gridbox over all the 1×1 km urban pixels in the modelling system. Mismatches due to differing land-sea masks at different resolutions have been solved by distributing the flux of a wrongly-so sea pixel over its neighbouring land pixels following knowledge of the local situation.

The emissions are also disaggregated in time and here a distinction is made between the "mobile" emissions (mostly road transport) and non-mobile emissions (industry, energy and small combustion and residential). For mobile emissions a diurnal cycle is assumed with no seasonal cycle where as for the non-mobile emissions a seasonal cycle is is assumed with no diurnal cycle. Both graphs in Fig. 6 show the relative contribution of that category to the emission. In the mobile emissions clearly a higher emission value can be seen during rush hours in the morning and evenings and almost no emission during night time. The shape of this graph is based upon work done by Wickert (2001) and Kuhlwein et al. (2002). For the non-mobile emissions a different pattern can be seen with higher emissions for Europe during wintertime as a result of higher heating rates.

2.5 Region

The simulations are performed for the RECAB summer campaign which was held between 8 and 28 July 2002. The experimental region comprises a big part of the centre of the Netherlands, measuring 70 km diagonally between the flux tower of Loobos and the tall tower of Cabauw. Figures 3 and 4 both show the location of both towers together with other observational sites (Haarweg-site in Wageningen and Harskamp) which were used during the campaign. These figures also show the land use cover and the soil map of the area. From these maps four major landscape units appear corresponding to the roman numbers on Fig. 3:

- hilly glacial deposits mainly covered by various forest types (evergreen needle leaf, deciduous broadleaf and mixed); maximum altitude 110 m above means sea level (area I);
- agricultural land dominated by a mixture of grassland and maize crops on mostly sandy soils in between the hilly glacial deposits (area II);
- very low lying, wet grassland on clay and/or peat soils, mostly along the major rivers to the south of the line Haarweg – Cabauw (area III);
- urban areas (bright red areas in Fig. 3).

The region exhibits a maritime temperate climate. During the campaign the local weather was rather unstable, cloudy and slightly colder and wetter than average. The maximum temperature dropped to values well below 20°C after three days in the campaign and only in the final days of the campaign the temperature started to rise strongly to maximum values of 25–30°C. This prolonged period of cold weather was accompanied with cloudy circumstances from time to time, leading to precipitation. At Loobos a total of 14.2 mm was measured during this period. During this period it was impossible for the aircrafts to do proper measurements and therefore flying days were limited to the starting days and ending days of the campaign.

BGD

5, 4161–4207, 2008

2.6 Observations

Campaign wise observations have been made of:

- exchange fluxes of CO_2 between land and atmosphere deploying a number of permanent (3) and mobile (1) eddy-correlation flux towers (see Table 3), as well as a low-flying eddy-correlation flux aircraft. Flux towers and the eddy-correlation flux aircraft compare well in magnitude and dynamics of all fluxes Gioli et al. (2004) although scatter is large in the latter;

- convective boundary layer (CBL) concentrations of CO_2 and other greenhouse gases, deploying flask-and continuous sampling from an aircraft, and continuous sampling from the tall tower at Cabauw.

Flying days during the campaign were on 15, 16, 23, 24, 25, 26 and 27 July with the last day in best meteorological conditions. On 15, 16, 24 and 27 July two return flights from Loobos to Cabauw were performed with the low-flying eddy-correlation flux aircraft and on 15, 16 and 27 July vertical profiles were taken in the morning and in the afternoon with the aircraft performing CBL measurements. This paper will focus on the first period of the summer campaign as for these days multiple observations are available to test the model.

3 Results and analyses

The results of the model will be compared with observations carried out during the RECAB summer campaign. First, a comparison will be made between station observations and simulated results focussing on the various fluxes between the land surface and atmosphere. Second, the observations carried out by the aircrafts are compared with model results. These will be divided into comparisons of vertical profiles of CO_2 concentrations and temperatures on one hand and comparisons of latent heat, sensible heat and CO_2-fluxes along paths flown by the low-flying flux aircraft on the other.

BGD

5, 4161–4207, 2008

Simulation of carbon exchange using a regional model

H. W. Ter Maat and R. W. A. Hutjes

Model output is stored every hour and only output from the smallest grid, which has a resolution of 4 km, is presented. For comparison with the observational tower data, model output was taken from the grid point nearest to the observational site. Aircraft data was compared against interpolated model output using bi-linear interpolation.

3.1 Validation against station observations

In the first set of graphs we compare simulated fluxes at grid and patch level with observed fluxes at the tower sites. Each grid box of a model can represent more than one land use class, so-called tile-approach for sub-grid variability. We compare fluxes for the grid box nearest to the tower-site, and for the land cover class most resembling that observed at the tower site. For the grid cell including the Loobos pine forest site we find the following distribution of land use classes 44% forest, 44% grassland and 11% agriculture. The same grid cell also covers the Harskamp maize site. The grid cell containing the Cabauw grass site contains 100% grassland. The Haarweg (grassland in reality) grid cell contains 56% grassland, 33% agriculture and 11% urban area.

Figure 7 shows a comparison of observed and simulated incoming shortwave radiation ($\mathrm{W\,m^{-2}}$) for the Loobos site. For a number of days the agreement is very good, but for other days the model underestimates the global radiation. This is mostly due to a misrepresentation of the exact location and timing of the passage of various simulated cloud systems as the local weather was rather unstable as was mentioned before. Next, it seems that the simulated cloud cover transmits less radiation than in reality. Comparisons with other sites show the same results with a reasonable estimation of the incoming shortwave radiation. Overall the fluxes are underestimated by 25% with a correlation coefficient (r^2) of 0.6.

The same patterns can be found in the comparison between observations and model for the latent heat flux ($\mathrm{W\,m^{-2}}$). Figure 8 shows the observed and simulated latent heat flux for the complete summer campaign for the three main land use types: needle leaf forest (Loobos), grassland (Haarweg) and agricultural land (Harskamp). In general, the agreement for the forest and agricultural site is good, but for the grassland site the

BGD

5, 4161–4207, 2008

Title Page

Abstract Introduction

Conclusions References

Tables Figures

◂◂ ▸▸

◂ ▸

Back Close

Full Screen / Esc

Printer-friendly Version

Interactive Discussion

evaporation is often underestimated. This is for a large part caused by the underestimation of the shortwave radiation and therefore available energy by the model.

Simulated CO_2 fluxes (μmol m^{-2} s^{-1}) are compared with observations in Fig. 9. Only the Loobos and Haarweg site are displayed here as the CO_2 observations of the Harskamp site were limited in this period due to problems with the measurement instrument. However, for this site from the few data available we can conclude that the simulated CO_2 uptake of the maize is underestimated as a result of the generic parameter values obtained from Knorr (2000). This lack of observational data made it impossible to derive correct parameter values for the maize-site in Harskamp. Another complication is that PELCOM does not discriminate between specific crops in the PELCOM classes of rain fed or irrigated arable land (see Fig. 3). The simulated CO_2 flux for Loobos and Haarweg follow the observed CO_2 flux quite nicely. Except for some midday peaks for Loobos the assimilation looks reasonable. The night time respiration at the grassland site is underestimated by the model, but for the forest site the respiration is simulated in accordance with the measurements. At 19 July the model simulates for both sites a CO_2 flux with a weaker photosynthesis than the observations show. This day is characterized by a shortwave radiation which is limited by cloud cover in both simulations and observations (see Fig. 7). Again, the effect of reduced shortwave radiation on the CO_2 flux appears stronger in the model than in the observations.

3.2 Validation against aircraft observations

Figures 10 and 11 respectively show spatially explicit simulated latent heat and carbon fluxes in comparison with those observed from the flux aircraft, for 16 July around 07:00 UTC and 11:00 UTC (09:00 and 13:00 LT). The top panel of both figures show the spatially patterns of the simulated fluxes combined with an overlay of the flight track of the flights. The lower panel shows a comparison between simulated and observed fluxes in terms of both their absolute values and anomalies of the flux which is defined as the deviation from the average of the total flight track. These are also normalized by the standard deviation of the data points

$$F' = \frac{F - \overline{F}}{\sigma} \tag{1}$$

Figures 10 and 11 demonstrate that the wind direction and speed (displayed as wind vectors) are simulated in accordance with the observations from the aircraft. Comparing spatially explicit simulated and observed fluxes shows that in general simulated latent heat fluxes are too low relative to observed (Fig. 10). Table 4 shows the average latent heat flux per major landscape unit (I, II and III in Fig. 3) for both flights on 16 July. The difference between observed and simulated fluxes for all landscape units is notably large for the early morning flight on 16 July with fluxes underestimated on average for the whole flight track by almost 150 W m^{-2}. This is not in line with the validation on station level (see Fig. 8) where latent heat flux is reasonably simulated by the model on 16 July. The average simulated latent heat flux for the second flight on 16 July is more in line with observation with a simulated latent heat flux of 174.8 W m^{-2} compared to an observed flux of 219.0 W m^{-2}. This underestimation is detected in all landscape units but is most apparent for landscape unit III (wet grassland along the river). However, the standard deviation in observed latent heat fluxes is so large (first flight: 110 W m^{-2}, second flight: 137 W m^{-2}) that it is almost difficult to compare the aircraft observations with the simulated results for a decent validation. This holds true for all latent heat flux observations of aircraft measurements during the observational campaign. Especially mid-day flights around local noon often exhibit a standard deviation that is larger than the average flux. For morning and afternoon flights the variation is generally somewhat reduced.

The spatially simulated CO_2-fluxes are compared in Fig. 11 with the observations from the aircraft. From the comparison between simulated trends in results and observations a similar pattern can be seen, with a larger uptake for the Veluwe area (beginning and ending of the graph in the lower panel of Fig. 11). The top panel of both figures show absolute values of CO_2-fluxes where the blue colour coding reflects the uptake of CO_2 by the vegetation and the red colour coding the release of CO_2

through emission or respiration. Simulated spatial variation in CO_2-fluxes is dominated by the contrast between anthropogenic sources over urban areas and biospheric sinks over rural areas. Since the aircraft flight path was obligatory avoiding build-up areas (for safety reasons), it could not capture the largest contrasts in this environment. The landscape feature that is rather consistently resolved in both model and observations and in both heat and CO_2-fluxes is the large forest area of the Veluwe, located in the eastern part of the domain. Averaged along the flight track (Table 5) we see that the simulated CO_2-flux is comparable with the observed flux for the early morning flight. The observations show only a stronger downward flux of CO_2 compared to the simulated values above the forested area. This is partly compensated by a stronger downward flux of CO_2 above the wet grassland along the rivers. Due to the near-absence of turbulent diffusion in the early morning at levels above the surface both latent heat and CO_2 fluxes at flight level are underestimated by the model as is shown by the line graphs in both Figs. 10 and 11. Looking at the trends of CO_2-fluxes along the flight path the model captures the various landscape elements nicely with negative fluxes simulated at the end of the return flight of the airplane.

During the observational also campaign profiles of various variables have been measured using an aircraft. Figures 12 and 13 show the comparisons between, respectively, potential temperature (K) and CO_2 concentration (ppm) for four timeslots during the 16 July when the profiles were measured. The profiles are measured at various locations in the central Netherlands. Comparing potential temperature profiles we can observe that the fit between simulated an observed profiles is improving during the day. The profiles measured in the vicinity of Cabauw (red – morning and blue – afternoon) show that in the morning the lower part of the atmosphere is simulated with lower potential temperature than observed. This is also true for the morning profile measured near the Loobos observational tower. The afternoon profile near Cabauw shows that the potential temperature in the lower atmosphere is simulated in accordance with measurements. The model tends to underestimate potential temperature by 1–2 K higher up in the planetary boundary layer (PBL). Simulated PBL height on

BGD

5, 4161–4207, 2008

16 July stays somewhat behind reality – respectively 1200 m vs. 1500 m maximum. This has its direct effect on the simulated CO_2 concentration with a lower PBL height leading to higher CO_2 concentration. Although the concentration is in general overestimated by the model for this particular day, the trends are simulated well by the model with a typical early morning CO_2 profile, (CO_2 trapped in the lower part of the atmosphere) developing in a well-mixed profile in the afternoon. Figure 14 shows the time series of the observed and simulated CO_2 concentration at the 60 m level at Cabauw. In general the model is capturing the dynamics in the concentration good, but is also cleaner than the observations justify, especially during night time. This contrasts with the results from the concentration profile where the model overestimated the CO_2 concentration. Figure 14 shows that this is typical for the morning of 16 July, but also for other mornings at the end of the simulation.

3.3 Sensitivity experiments

To explore some controlling factors determining carbon dioxide concentration two sensitivity experiments were performed for the first three days of the period. In the first simulation anthropogenic (urban) fluxes were increased by 20% and in the second simulation a 20% increase was given to the biogenic (all vegetation classes) fluxes. Results of both sensitivity experiments were subsequently compared with the standard experiment. This analysis suggest that the western part of the Netherlands, densely populated, is more sensitive to a change of 20% in anthropogenic emissions than in biogenic emissions/uptake leading to a change of more than 8 ppm in the CO_2 concentration near the surface in the anthropogenic sensitivity experiment (Fig. 15). The influence of this change is only felt close to the surface and will only have its impact in the lower 200 m of the atmosphere. The relative contribution of the biogenic sources (maximum change: 1.6 ppm, not shown) is smaller than the relative contribution of the anthropogenic emissions. For the eastern part (surroundings of the Veluwe) the story is different. In the vicinity of the Loobos tower it appears that the 20% change in both anthropogenic and biogenic fluxes account for an equal change in CO_2 con-

BGD
5, 4161–4207, 2008

centration during night time resulting from higher anthropogenic emissions and higher respiration of the forest (Fig. 16). During daytime the change in CO_2 concentration at Loobos resulting from different emissions is smaller than at Cabauw. Higher uptake of the forested contributes slightly more to the CO_2 concentration as the contribution of a more assimilating forest outweighs this of the few cities on and around the Veluwe.

4 Discussion and conclusions

The coupled regional model (RAMS-SWAPS-C) is in general doing a decent job in simulating results close to reality. For the simulated period the comparison between station observations and model output looked very promising for the grass and forest sites. Latent heat flux for the agricultural site was simulated well but it appeared that the CO_2-flux, especially photosynthesis, was underestimated significantly. This asks for observations above various land use types so that parameters which describe, amongst others, the carbon exchange of the vegetation (maize in this case) can be better estimated. This approach was taken during the CERES campaign, which was held in the early summer of 2005 (Dolman et al., 2006), and campaigns which were set up within the framework of the Netherlands research programme “Climate changes spatial planning” (Kabat et al., 2005). These initiatives will provide the modelling community with a multitude of station observations for various land use types. In addition, land use maps should also account for this vegetation class if the difference with other vegetations is significantly large.

Another shortcoming in the comparison between the model and the observations is that the radiation is blocked too strongly by the model leading, in cloudy situations, to underestimation of the incoming shortwave radiation at the surface by the model. This in turn has its effect on the energy balance near the surface and the simulated CO_2-flux. Next to this “blocking” effect the location and timing of cloud systems appeared to be important during the simulated period as this period of intense measurements was characterized by unstable, windy weather with a multitude of cloud systems of

BGD
5, 4161–4207, 2008

H. W. Ter Maat and R. W. A. Hutjes

Title Page
Abstract | Introduction
Conclusions | References
Tables | Figures
◀◀ | ▶▶
◀ | ▶
Back | Close
Full Screen / Esc
Printer-friendly Version
Interactive Discussion

various scales passing over the Netherlands. As might be expected, the model is able to capture the large-scale systems, but has problems with the smaller scale features.

Aircraft observed fluxes of latent heat flux during the observational campaign exhibited a lot of scatter with standard deviations being sometimes larger than the average flux. This could not be related to particular landscape features, but is mainly a result of meteorological conditions and eddies of various sizes leading to high variation in the aircraft observations. This large scatter in aircraft observed fluxes makes it difficult to rightly validate spatially simulated fields of latent heat flux. Simulated spatial variation in fluxes for the simulated period is generally caused by clouds (and its blocking of solar radiation) and is larger than variations that can be linked to known surface heterogeneities.

Spatially simulated carbon fluxes were compared against aircraft observations and the results showed that the simulated trends in carbon exchange followed the observed trends although not as profound as observations showed. The simulated absence of turbulent diffusion is apparent as the CO_2-fluxes at flight level are close to zero even when a significant uptake at the surface is simulated. Even though the observational aircraft try to fly as low as regulations allowed in the Netherlands, the contribution from neighbouring areas that might be a part of the footprint seen by the aircraft can not be excluded. The interpretation of aircraft observations asks for more studies using approaches of footprint modelling. According to Garten et al. (2003) a serious shortcoming in simple footprint models, which are based on the Gaussian plume approach, is the inability to predict how quickly real clouds move and redistribute themselves vertically under particular meteorological conditions. Therefore, a lagrangian model combined with the meteorological dynamics of a regional atmospheric model (eulerian) may be one approach that can help to interpret aircraft data better (Hutjes et al., 2008). The lagrangian approach will be helpful to interpret profiles and the various sources or sinks that contribute to changes in scalar profiles, whereas the eulerian approach will be used for the fluxes.

The various profiles measured during the first period of the campaign showed that the model underestimates potential temperature especially in the morning. The convective boundary layer dynamics seem to be reproduced well by the model. However, fine scale structures in observed scalar profiles cannot be captured with the current vertical resolution of the model. From the station validation we can also see that during most mornings in the simulation the depletion of CO_2 at the lower levels is slower in the model than in the observations. From the station validation of the CO_2 concentration (Fig. 14) the influence of the sea might be an important factor for the concentrations simulated near the coastal strip of the Netherlands. One of the shortcomings of the present modelling system is the coarse resolution of the partial pressure of CO_2 within the sea and the values that were derived for the North Sea west and northwest of the Netherlands. According to Hoppema (1991) and Thomas et al. (2004) there is a strong gradient in the North Sea near the Dutch coastal strip with absolute values of the CO_2 partial pressure also being more dynamical in time than the values from Takahashi et al. (1997) suggest. Seasonal fields observations show that the North Sea acts as a sink for CO_2 throughout the year except for the summer months in the southern region of the North Sea. Figure 5 shows that the modelling system lacks these dynamics in $\delta p CO_2$. As a result in the case of strong winds blowing from west/northwestern directions relative low simulated CO_2 air will penetrate inland compared to the seasonal fields observations in summer months.

The validation of the vertical profiles indicates that the depth of the boundary layer is not well represented and is underestimated by 100–200 m by the model. de Arellano et al. (2004) assessed the importance of the entrainment process for the distribution and evolution of carbon dioxide in the boundary layer. They also showed that the CO_2 concentration in the boundary layer is reduced much more effectively by the ventilation with entrained air than by CO_2 uptake by the vegetation. In the turbulent parameterization (Mellor-Yamada) of the atmospheric model we found that the entrainment process is poorly represented leading to a higher simulated CO_2 concentration in most of the vertical profile. For future modelling experiments it is necessary to focus on the importance of entrainment processes in turbulent parameterizations.

BGD

5, 4161–4207, 2008

From the results of the sensitivity experiments we conclude that the response of [CO_2] to these variations is larger at Cabauw than at Loobos. We also conclude that it is possible to determine the cause of an observed change in CO_2 concentration in terms of sources and sinks in the vicinity of an observational site. This is complimentary to the work described by Vermeulen et al. (2006) who concluded that "inverse methods (. . .) are suitable to be applied in deriving independent estimates of greenhouse gas emissions using Source-Receptor relationships". Given this approach an observed change in CO_2 concentration can be related to a certain greenhouse gas emission from a certain land use in the vicinity of the observational site. This study follows closely the recommendations given by Geels et al. (2004) for future modeling work of improved high temporal resolution (at least daily) surface biosphere, oceanic and anthropogenic flux estimates as well as high vertical and horizontal spatiotemporal resolution of the driving meteorology. It also suggest that to resolve 20% flux difference you either need to measure close to the surface or very precise.

This paper tried to determine what factors are controlling the content of carbon dioxide for a region covering a large part of the Netherlands. This was achieved using a regional model coupled to a detailed land-surface model and using various observations ranging from station to aircraft measurements. The region used for this study is characterized by a strong heterogenic appearance of various land use alternated with cities/villages of various sizes. It can be concluded that at the local scale these cities play an important role in the amount of carbon dioxide in the atmosphere. This is illustrated in Fig. 17 showing the transport of "rich CO_2" air mass originating from the cities. The forest at the Veluwe can play a part in decreasing the atmospheric content of carbon dioxide. To what extent these counteracting signals play a role has to be investigated further more. At a larger scale, the influence of the cleaning effect of the sea proved to be important to simulate the CO_2 concentrations more realistically. The effect of better representations of the partial pressure-fields of CO_2 for the North Sea on the simulated CO_2 concentration inland remains a subject needing further research.

Acknowledgements. This study is supported by the projects RECAB (EVK2-CT-1999-00034) and CarboEurope-IP project (GOCE-CT2003-505572) funded by the European Commission and by the Netherlands research program "Climate changes Spatial Planning". Furthermore, the authors want to express their thanks to all those who worked hard to collect the data in the field: Alex Vermeulen (ECN, Petten, the Netherlands), Fred Bosveld (KNMI, De Bilt, the Netherlands), Wilma Jans and Jan Elbers (Alterra-WUR, Wageningen, the Netherlands). For helping us with the interpretation and post-processing of the aircraft data we would like to thank Franco Miglietta and Beniamino Gioli (Ibimet, Florence). ECMWF is acknowledged for providing meteorological analysis and reanalysis data.

References

Ashby, M.: Modelling the water and energy balances of Amazonian rainforest and pasture using Anglo-Brazilian Amazonian climate observation study data, Agr. Forest Meteorol., 94, 79–101, 1999.

Bakwin, P. S., Tans, P. P., Zhao, C. L., Ussler, W., and Quesnell, E.: Measurements of Carbon-Dioxide on a Very Tall Tower, Tellus B, 47, 535–549, 1995.

Betts, A. K., Desjardins, R. L., and Macpherson, J. I.: Budget Analysis of the Boundary-Layer Grid Flights During FIFE 1987, J. Geophys. Res.-Atmos., 97, 18 533–18 546, 1992.

Collatz, G. J., Ribas Carbo, M., and Berry, J. A.: Coupled photosynthesis-stomatal conductance model for leaves of C4 plants, East Melbourne : Commonwealth Scientific and Industrial Research Organization, Aust. J. Plant Physiology, 19, 519–539, 1992.

Cotton, W. R., Pielke, R. A., Walko, R. L., Liston, G. E., Tremback, C. J., Jiang, H., McAnelly, R. L., Harrington, J. Y., Nicholls, M. E., Carrio, G. G., and McFadden, J. P.: RAMS 2001: Current status and future directions, Meteorol. Atmos. Phys., 82, 5–29, 2003.

Culf, A. D., Fisch, G., Malhi, Y., and Nobre, C. A.: The influence of the atmospheric boundary layer on carbon dioxide concentrations over a tropical forest, Agr. Forest Meteorol., 85, 149–158, 1997.

de Arellano, J. V. G., Gioli, B., Miglietta, F., Jonker, H. J. J., Baltink, H. K., Hutjes, R. W. A., and Holtslag, A. A. M.: Entrainment process of carbon dioxide in the atmospheric boundary layer, J. Geophys. Res.-Atmos., 109(D18), D18110, doi:10.1029/2004JD004725, 2004.

Denning, A. S., Fung, I. Y., and Randall, D.: Latitudinal Gradient of Atmospheric CO_2 Due to Seasonal Exchange with Land Biota, Nature, 376, 240–243, 1995.

Denning, A. S., Takahashi, T., and Friedlingstein, P.: Can a strong atmospheric CO_2 rectifier effect be reconciled with a "reasonable" carbon budget?, Tellus B, 51, 249–253, 1999.

Derwent, R. G., Ryall, D. B., Manning, A., Simmonds, P. G., O'Doherty, S., Biraud, S., Ciais, P., Ramonet, M., and Jennings, S. G.: Continuous observations of carbon dioxide at Mace Head, Ireland from 1995 to 1999 and its net European ecosystem exchange, Atmos. Environ., 36, 2799–2807, 2002.

Dolman, A. J.: A Multiple-Source Land-Surface Energy-Balance Model for Use in General-Circulation Models, Agr. Forest Meteorol., 65, 21–45, 1993.

Dolman, A. J., Noilhan, J., Durand, P., Sarrat, C., Brut, A., Piguet, B., Butet, A., Jarosz, N., Brunet, Y., Loustau, D., Lamaud, E., Tolk, L., Ronda, R., Miglietta, F., Gioli, B., Magliulo, V., Esposito, M., Gerbig, C., Korner, S., Glademard, R., Ramonet, M., Ciais, P., Neininger, B., Hutjes, R. W. A., Elbers, J. A., Macatangay, R., Schrems, O., Perez-Landa, G., Sanz, M. J., Scholz, Y., Facon, G., Ceschia, E., and Beziat, P.: The CarboEurope regional experiment strategy, B. Am. Meteorol. Soc., 87, 1367–1379, 2006.

Flatau, P. J., Tripoli, G. J., Verlinde, J., and Cotton, W. R.: The CSU-RAMS cloud microphysical module: General theory and code documentation, Colorado State Univ., Fort Collins, Colorado, 451, 88 pp., 1989.

Garten, J. F., Schemm, C. E., and Croucher, A. R.: Modeling the transport and dispersion of airborne contaminants: A review of techniques and approaches, Johns Hopkins Apl Technical Digest, 24, 368–375, 2003.

Geels, C., Doney, S. C., Dargaville, R., Brandt, J., and Christensen, J. H.: Investigating the sources of synoptic variability in atmospheric CO_2 measurements over the Northern Hemisphere continents: a regional model study, Tellus B, 56, 35–50, 2004.

Gerbig, C., Lin, J. C., Wofsy, S. C., Daube, B. C., Andrews, A. E., Stephens, B. B., Bakwin, P. S., and Grainger, C. A.: Toward constraining regional-scale fluxes of CO_2 with atmospheric observations over a continent: 2. Analysis of COBRA data using a receptor-oriented framework, J. Geophys. Res.-Atmos., 108(D24), 4757, doi:10.1029/2003JD003770, 2003.

Gioli, B., Miglietta, F., De Martino, B., Hutjes, R. W. A., Dolman, H. A. J., Lindroth, A., Schumacher, M., Sanz, M. J., Manca, G., Peressotti, A., and Dumas, E. J.: Comparison between tower and aircraft-based eddy covariance fluxes in five European regions, Agr. Forest Meteorol., 127, 1–16, 2004.

Global Soil Data Task Group, Global Gridded Surfaces of Selected Soil Characteristics (IGBP-DIS), [Global Gridded Surfaces of Selected Soil Characteristics (International Geosphere-Biosphere Programme – Data and Information System)], Data set, Available on-line [http://www.daac.ornl.gov] from Oak Ridge National Laboratory Distributed Active Archive Center, Oak Ridge, Tennessee, USA, doi:10.3334/ORNLDAAC/569, 2000.

Gurney, K. R., Law, R. M., Denning, A. S., Rayner, P. J., Baker, D., Bousquet, P., Bruhwiler, L., Chen, Y. H., Ciais, P., Fan, S., Fung, I. Y., Gloor, M., Heimann, M., Higuchi, K., John, J., Maki, T., Maksyutov, S., Masarie, K., Peylin, P., Prather, M., Pak, B. C., Randerson, J., Sarmiento, J., Taguchi, S., Takahashi, T., and Yuen, C. W.: Towards robust regional estimates of CO_2 sources and sinks using atmospheric transport models, Nature, 415, 626–630, 2002.

Hanan, N. P., Kabat, P., Dolman, A. J., and Elbers, J. A.: Photosynthesis and carbon balance of a Sahelian fallow savanna, Glob. Change Biol., 4, 523–538, 1998.

Hanan, N. P.: Enhanced two-layer radiative transfer scheme for a land surface model with a discontinuous upper canopy, Agr. Forest Meteorol., 109, 265–281, 2001.

Harrington, J. Y.: The effects of radiative and microphysical processes on simulated warm and transition season arctic stratus, Ph.D. thesis, Colorado State University, Fort Collins, CO, USA, 289 pp., 1997.

Hoppema, J. M. J.: The Seasonal Behavior of Carbon-Dioxide and Oxygen in the Coastal North-Sea Along the Netherlands, Neth. J. Sea Res., 28, 167–179, 1991.

Hutjes, R. W. A., Vellinga, O., Gioli, B., and Miglietta, F.: Disaggregation of airborne flux measurements using footprint analysis, Biogeosciences, to be submitted, 2008.

Janssens, I. A., Freibauer, A., Ciais, P., Smith, P., Nabuurs, G. J., Folberth, G., Schlamadinger, B., Hutjes, R. W. A., Ceulemans, R., Schulze, E. D., Valentini, R., and Dolman, A. J.: Europe's terrestrial biosphere absorbs 7 to 12% of European anthropogenic CO_2 emissions, Science, 300, 1538–1542, 2003.

Kabat, P., Hutjes, R. W. A., and Feddes, R. A.: The scaling characteristics of soil parameters: From plot scale heterogeneity to subgrid parameterization, J. Hydrol., 190, 363–396, 1997.

Kabat, P., van Vierssen, W., Veraart, J., Vellinga, P., and Aerts, J.: Climate proofing the Netherlands, Nature, 438, 283–284, 2005.

Knorr, W.: Annual and interannual CO_2 exchanges of the terrestrial biosphere: process-based simulations and uncertainties, in: GTCE-LUCC Special Section: Papers resulting from the Joint Open Science Conference of the IGBP Global Change and Terrestrial Ecosystems Project and the IGBP-IHDP Land Use and Cover Change Project, held in Barcelona, Spain,

March 1998, 224, 225–252, 2000 (in English).
Kuhlwein, J., Wickert, B., Trukenmuller, A., Theloke, J., and Friedrich, R.: Emission-modelling in high spatial and temporal resolution and calculation of pollutant concentrations for comparisons with measured concentrations, Atmos. Environ., 36, S7–S18, 2002.
Lloyd, J., Grace, J., Miranda, A. C., Meir, P., Wong, S. C., Miranda, H. S., Wright, I. R., Gash, J. H. C., and McIntyre, J.: A simple calibrated model of Amazon rainforest productivity based on leaf biochemical properties, Oxford, Blackwell Scientific Publishers, Plant Cell Environ., 18, 1129–1145, 1995.
Marquardt, D. W.: An Algorithm For Least-Squares Estimation Of Nonlinear Parameters, J. Soc. Ind. Appl. Math., 11, 431–441, 1963.
Mellor, G. L. and Yamada, T.: Development of a turbulence closure model for geophysical fluid problems, Rev. Geophys. Space Ge., 20, 851–875, 1982.
Mücher, C. A., Champeaux, H. L., Steinnocher, K. T., Griguoio, S., Wester, K., Heunks, C., Winiwater, W., Kressier, F. P. , Goutorbe, J. P., ten Brink, B., van Katwijk, V. F., Furberg, O., Perdigao, V., and Nieuwenhuis, G. H. A.: Development of a consistent methodology to derive land cover information on a European scale from Remote Sensing for environmental monitoring: The PELCOM report, Wageningen, ALTERRA, Green World Research, Alterra Report 178, CGI report 6, 178 pp., 2001.
Ogink-Hendriks, M. J.: Modeling surface conductance and transpiratio of an oak forest in The Netherlands, Agr. Forest Meteorol., 74, 99–118, 1995.
Olivier, J. G. J. and Berdowski, J. J. M.: Global emissions sources and sinks, in: The Climate System, edited by: Berdowski, J. J. M., Guicherit, R., and Heij, B. J., A. A. Balkema Publishers/Swets & Zeitlinger Publisher, Lisse, 33–78, 2001.
Pérez-Landa, G., Ciais, P., Gangoiti, G., Palau, J. L., Carrara, A., Gioli, B., Miglietta, F., Schumacher, M., Millán, M. M., and Sanz, M. J.: Mesoscale circulations over complex terrain in the Valencia coastal region, Spain - Part 2: Modeling CO_2 transport using idealized surface fluxes, Atmos. Chem. Phys., 7, 1851–1868, 2007a, http://www.atmos-chem-phys.net/7/1851/2007/.
Pérez-Landa, G., Ciais, P., Sanz, M. J., Gioli, B., Miglietta, F., Palau, J. L., Gangoiti, G., and Millán, M. M.: Mesoscale circulations over complex terrain in the Valencia coastal region, Spain - Part 1: Simulation of diurnal circulation regimes, Atmos. Chem. Phys., 7, 1835–1849, 2007b, http://www.atmos-chem-phys.net/7/1835/2007/.
Pielke, R. A., Cotton, W. R., Walko, R. L., Tremback, C. J., Lyons, W. A., Grasso, L. D., Nicholls,

M. E., Moran, M. D., Wesley, D. A., Lee, T. J., and Copeland, J. H.: A Comprehensive Meteorological Modeling System – Rams, Meteorol. Atmos. Phys., 49, 69–91, 1992.
Rayner, N. A., Parker, D. E., Horton, E. B., Folland, C. K., Alexander, L. V., Rowell, D. P., Kent, E. C., and Kaplan, A.: Global analyses of sea surface temperature, sea ice, and night marine air temperature since the late nineteenth century, J. Geophys. Res.-Atmos., 108(D14), 4407, doi:10.1029/2002JD002670, 2003.
Sarrat, C., Noilhan, J., Lacarrere, P., Donier, S., Lac, C., Calvet, J. C., Dolman, A. J., Gerbig, C., Neininger, B., Ciais, P., Paris, J. D., Boumard, F., Ramonet, M., and Butet, A.: Atmospheric CO_2 modeling at the regional scale: Application to the CarboEurope Regional Experiment, J. Geophys. Res.-Atmos., 112(D12), D12105, doi:10.1029/2006JD008107, 2007.
Soet, M., Ronda, R. J., Stricker, J. N. M., and Dolman, A. J.: Land surface scheme conceptualisation and parameter values for three sites with contrasting soils and climate, Hydrol. Earth Syst. Sci., 4, 283–294, 2000, http://www.hydrol-earth-syst-sci.net/4/283/2000/.
Spieksma, J. F. M., Moors, E. J., Dolman, A. J., and Schouwenaars, J. M.: Modelling evaporation from a drained and rewetted peatland, J. Hydrol., 199, 252–271, 1997.
Takahashi, T., Feely, R. A., Weiss, R. F., Wanninkhof, R. H., Chipman, D. W., Sutherland, S. C., and Takahashi, T. T.: Global air-sea flux of CO_2: An estimate based on measurements of sea-air $p$$CO_2$ difference, P. Natl. Acad. Sci. USA, 94, 8292–8299, 1997.
Ter Maat, H. W., Moors, E. J., Hutjes, R. W. A., and Dolman, A. J. Deriving land surface parameters for various pine forest sites, Agr. Forest Meteorol., submitted, 2007.
Thomas, H., Bozec, Y., Elkalay, K., and de Baar, H. J. W.: Enhanced open ocean storage of CO_2 from shelf sea pumping, Science, 304, 1005–1008, 2004.
Valentini, R., Matteucci, G., Dolman, A. J., Schulze, E. D., Rebmann, C., Moors, E. J., Granier, A., Gross, P., Jensen, N. O., Pilegaard, K., Lindroth, A., Grelle, A., Bernhofer, C., Grunwald, T., Aubinet, M., Ceulemans, R., Kowalski, A. S., Vesala, T., Rannik, Ü., Berbigier, P., Loustau, D., Guomundsson, J., Thorgeirsson, H., Ibrom, A., Morgenstern, K., Clement, R., Moncrieff, J., Montagnani, L., Minerbi, S., and Jarvis, P. G.: Respiration as the main determinant of carbon balance in European forests, Nature, 404, 861–865, 2000.
Van Wijk, M. T., Dekker, S. C., Bouten, W., Bosveld, F. C., Kohsiek, W., Kramer, K., and Mohren, G. M. J.: Modeling daily gas exchange of a Douglas-fir forest: comparison of three stomatal conductance models with and without a soil water stress function, Tree Physiol., 20, 115–122, 2000.

BGD
5, 4161–4207, 2008

H. W. Ter Maat and R. W. A. Hutjes

Vermeulen, A. T., Pieterse, G., Hensen, A., van Den Bulk, W. C. M., and Erisman, J. W.: COMET: a Lagrangian transport model for greenhouse gas emission estimation - forward model technique and performance for methane, Atmos. Chem. Phys. Discuss., 6, 8727–8779, 2006, http://www.atmos-chem-phys-discuss.net/6/8727/2006/.

Wanninkhof, R.: Relationship between Wind-Speed and Gas-Exchange over the Ocean, J. Geophys. Res.-Oceans, 97, 7373–7382, 1992.

Weiss, R. F.: Carbon dioxide in water and seawater: the solubility of a non-ideal gas, Mar. Chem., 2, 203–215, 1974.

Wickert, B.: Berechnung anthropogener Emissionen in Deutschland für Ozonsimulation – Modellentwicklung und Sensitivitätsstudien, PhD-thesis, Universität Stuttgart, Institut für Energiewirtschaft und Rationelle, 2001.

BGD

5, 4161–4207, 2008

Simulation of carbon exchange using a regional model

H. W. Ter Maat and R. W. A. Hutjes

Table 1. RAMS4.3 configuration.

Grids	1	2	3
dx, dy	48 km (83×83)	16 km (41×38)	4 km (42×42)
dt	50 s	16.7 s	16.7 s
dz	25–1000 m (35)		
Radiation	Harrington (1997)		
Topography	DEM USGS (∼1 km resolution)		
Land cover	PELCOM (Mücher et al., 2001)		
Land surface	SWAPS-C (Ashby, 1999; Hanan et al., 1998)		
Diffusion	Mellor/Yamada (Mellor and Yamada, 1982)		
Convection	Full microphysics package (Flatau et al., 1989)		
Forcing	ECMWF		
Nudging time scale	Lateral 1800 s		

BGD

5, 4161–4207, 2008

Simulation of carbon exchange using a regional model

H. W. Ter Maat and R. W. A. Hutjes

Table 2. Parameters for calculating the surface conductance and the net ecosystem exchange, classified by land use. $g_{s,max}$: maximum surface conductance (mm s^{-1}), $V_{m,ref}$: maximum catalytic capacity for Rubisco at canopy level (μmol m^{-2} s^{-1}) and α the intrinsic quantum use efficiency [–].

	$g_{s,max}$ (mm s^{-1})	$V_{m,ref}$ (μmol m^{-2} s^{-1})	α (–)	
Coniferous forest	33.4	55.8	0.0384	Optimized
Deciduous forest	51.0	41.0	0.0084	Ogink-Hendriks (1995), Knorr (2000)
Grass	25.9	91.96	0.0283	Optimized
Agricultural land	25.0	39.0	0.0475	Soet et al. (2000), Knorr (2000)

BGD
5, 4161–4207, 2008

Table 3. Description of operational sites during the RECAB campaign.

Site	Location	Landuse
Loobos	5.7439° E, 52.1667° N	Coniferous forest
Harskamp (mobile)	5.7157° E, 52.1491° N	Maize (Agricultural land)
Wageningen	5.628° E, 51.977° N	Grassland
Cabauw	4.927° E, 51.971° N	Grassland

BGD

5, 4161–4207, 2008

Simulation of carbon exchange using a regional model

H. W. Ter Maat and R. W. A. Hutjes

Table 4. Averaged latent heat fluxes along the flightpath for both flights on 16 July 2002. The three regions (see text) are referred to according to their roman number. flux atm represents the simulated flux at the same level as the flightpath, whereas flux sfc represents the simulated flux at the land surface below the flightpath.

16/07 1st flight	I	II	III	flightpath
average observation	141.7	140.7	179.1	163.3
average flux atm	43.4	14.0	1.5	12.4
average flux sfc	73.7	60.6	53.6	59.5
16/07 2nd flight	**I**	**II**	**III**	**flightpath**
average observation	185.4	199.6	243.4	219.0
average flux atm	155.6	173.3	181.9	174.8
average flux sfc	249.6	216.1	217.9	223.2

BGD
5, 4161–4207, 2008

H. W. Ter Maat and R. W. A. Hutjes

Table 5. Averaged CO_2 fluxes along the flightpath for both flights on 16 July 2002. The three regions (see text) are referred to according to their roman number.

16/07 1st flight	I	II	III	flightpath
average observation	−7.56	0.19	3.23	0.39
average flux atm	−0.59	1.45	0.71	0.70
average flux sfc	−8.74	−3.07	−3.51	−4.27
16/07 2nd flight	**I**	**II**	**III**	**flightpath**
average observation	−7.85	−9.16	−8.40	−8.44
average flux atm	−4.51	−1.77	0.05	−1.32
average flux sfc	−10.92	−5.10	−6.98	−7.23

BGD

5, 4161–4207, 2008

Simulation of carbon exchange using a regional model

H. W. Ter Maat and R. W. A. Hutjes

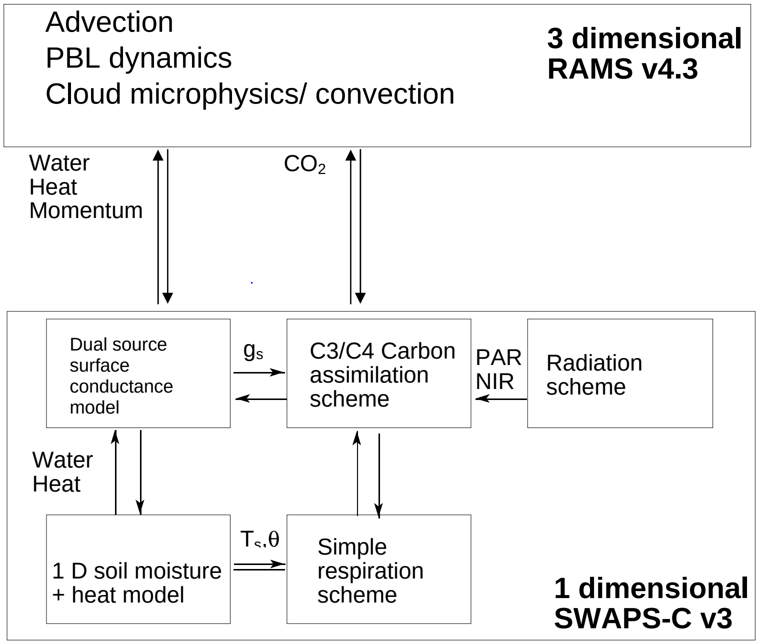

Fig. 1. Schematization of the coupling between RAMS and SWAPS-C. The main interactions between submodels is also given together with the variables with g_s – surface conductance, T_s – surface temperature, θ – soil moisture, PAR – photosynthetically active radiation, NIR – near infrared radiation.

BGD
5, 4161–4207, 2008

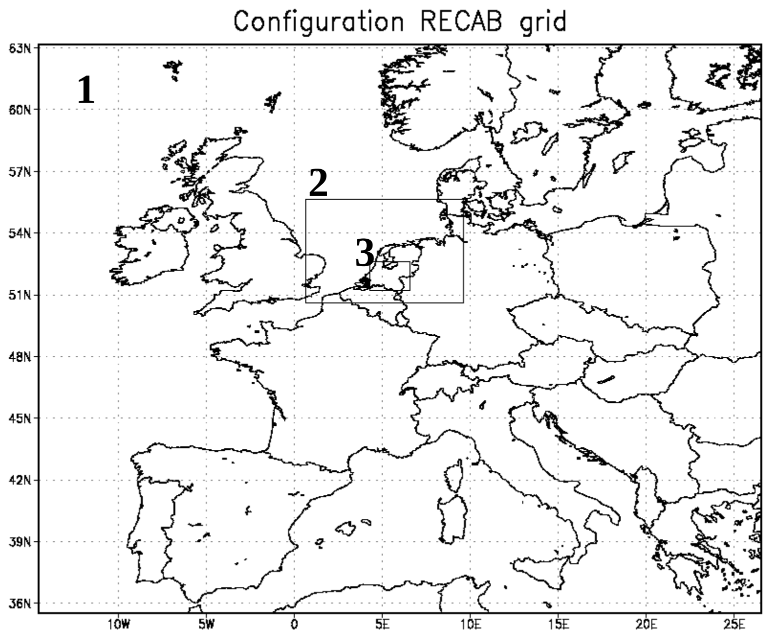

Fig. 2. Configuration of the modelling domain. Boxes and numbers illustrate the three grids.

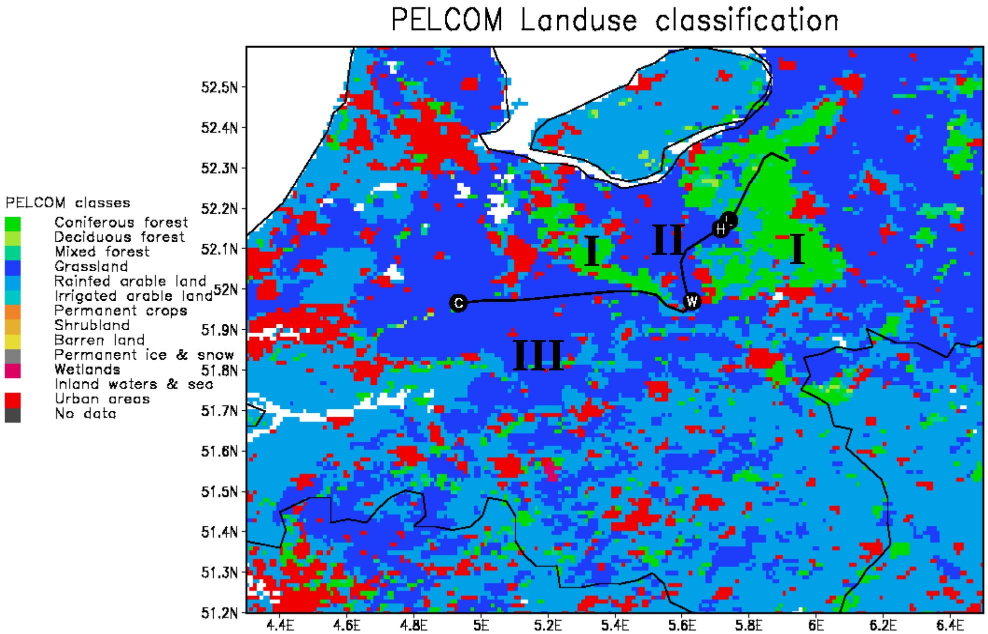

Fig. 3. Land cover classification (based on PELCOM) for the smallest grid in the domain. Along the flighttrack (given as a black line) the location of the observational sites are also given: C – Cabauw; W – Haarweg, Wageningen; H – Harskamp; L – Loobos. The roman numbers correspond to the areas described in the description of the region.

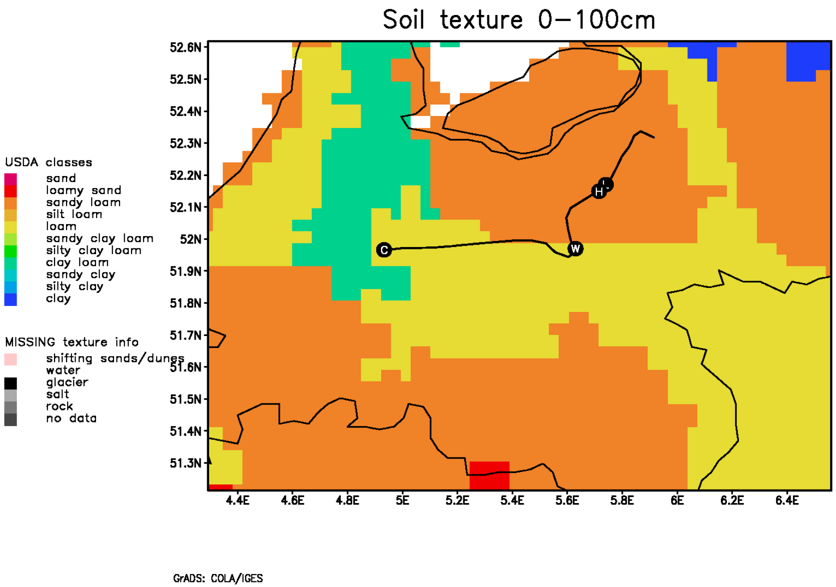

Fig. 4. Soil classification (depth 0–100 cm) for the smallest grid in the domain. Along the flighttrack (given as a black line) the location of the observational sites are also given: C – Cabauw; W – Haarweg, Wageningen; H – Harskamp; L – Loobos.

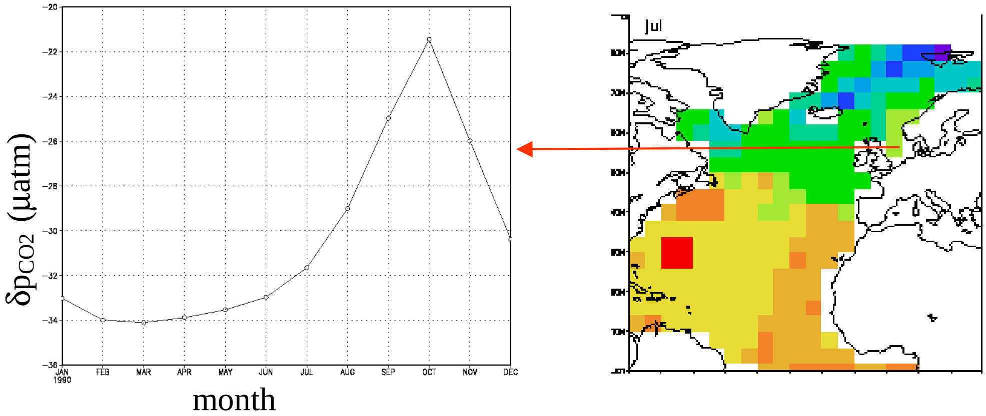

Fig. 5. Monthly dynamics of $\delta p\mathrm{CO}_2$ (μatm; 1 atm=1.01 325 Pa) as a timeseries for a pixel in the North Sea (left panel). Right panel shows the spatial representation of $\delta p\mathrm{CO}_2$ for the Atlantic Ocean.

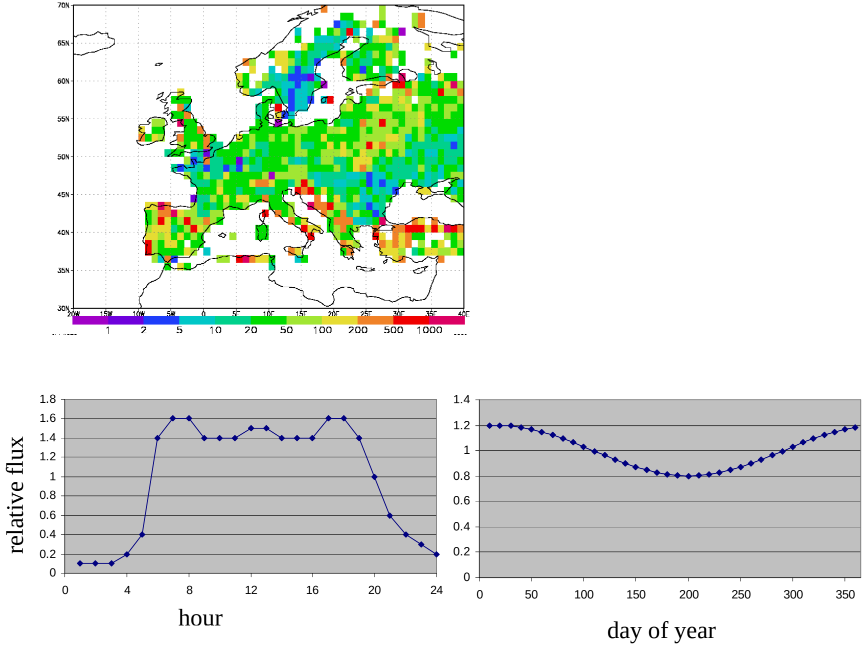

Fig. 6. Anthropogenic emissions (terrestrial only) as CO_2 flux in $\mu mol\, m^{-2}\, s^{-1}$ from EDGAR database version 3.2 (top). Lower panel shows the disaggregation of these emissions in time for mobile emissions (left) and for non-mobile emissions (right). Note that the emission is per m^2 urban area per pixel.

BGD

5, 4161–4207, 2008

Simulation of carbon exchange using a regional model

H. W. Ter Maat and R. W. A. Hutjes

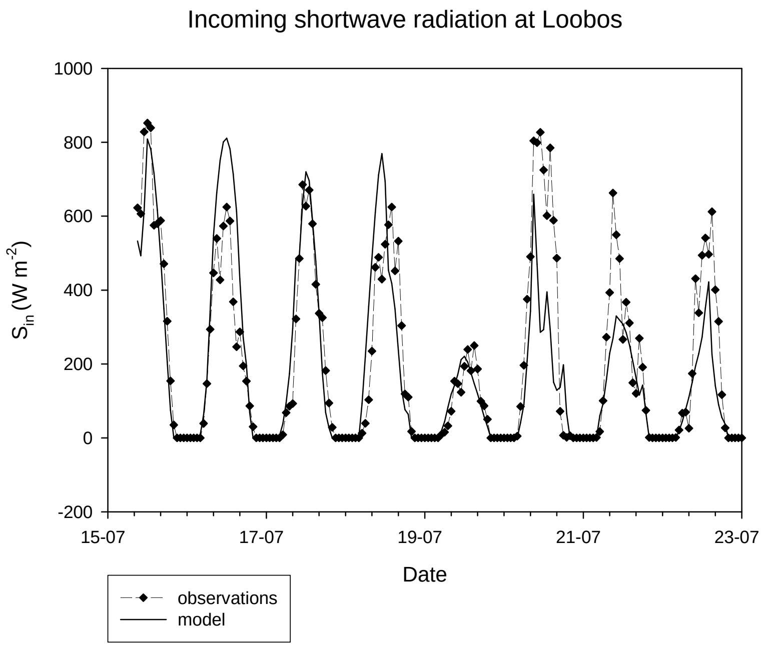

Fig. 7. Comparison of observed and simulated global radiation fluxes (W m^{-2}) at the Loobos site. Diamonds and dotted lines: observed values. Orange lines simulated at a gridpoint nearest to the Loobos site and representing the appropriate tile.

BGD

5, 4161–4207, 2008

Title Page
Abstract | Introduction
Conclusions | References
Tables | Figures
◀| |▶
◀ ▶
Back | Close
Full Screen / Esc
Printer-friendly Version
Interactive Discussion

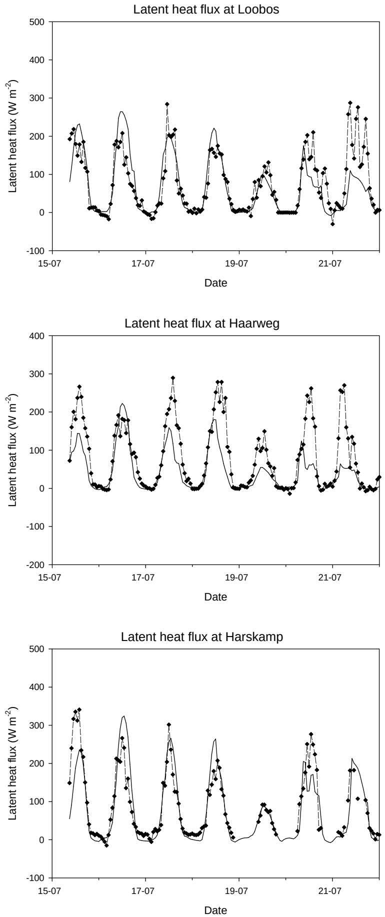

Fig. 8. Comparison of observed and simulated latent heat fluxes ($W\,m^{-2}$) for Loobos (top), Haarweg (middle) and Harskamp (bottom). Diamonds and dotted lines: observed values; orange lines simulated at a gridpoint nearest to the observational site and representing the appropriate tile.

BGD
5, 4161–4207, 2008

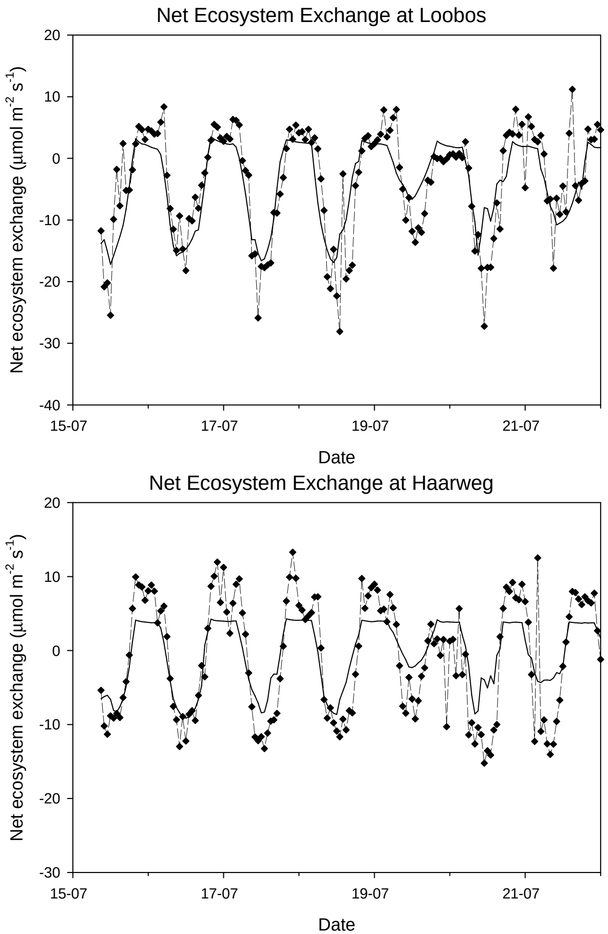

Fig. 9. Comparison of observed and simulated carbon fluxes (μmol m^{-2} s^{-1}) for Loobos (top) and Haarweg (bottom). Diamonds and dotted lines: observed values; orange lines simulated at a gridpoint nearest to the observational site and representing the appropriate tile.

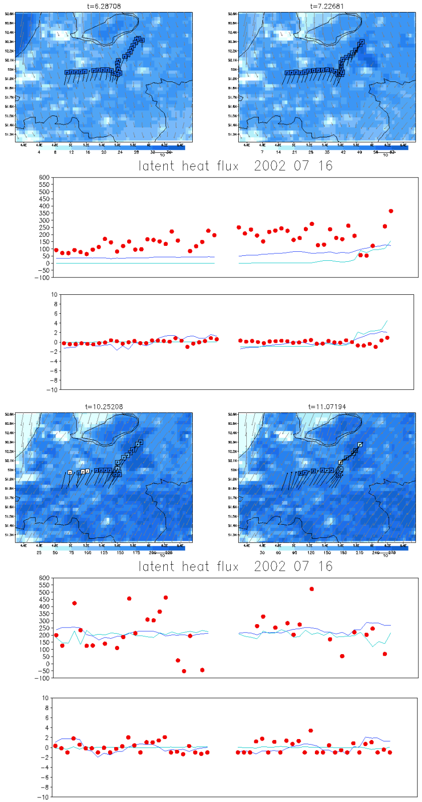

Fig. 10. Spatial comparison of latent heat fluxes ($W\,m^{-2}$) against aircraft observations, for the flights on 16 July 2002 (top: 06:28 UTC, 07:22 UTC; bottom: 10:25 UTC, 11:07 UTC). The maps show simulated flux fields at the surface and wind vectors (gray). Superimposed on that is the flight track with observed fluxes (squares) in the same colour coding as the background map, aircraft observed windvectors (black). The lower plots shows the aircraft observed fluxes (red dots), simulated fluxes at the surface (dark blue) and at flying altitude (light blue) in terms of both their absolute values and anomalies of the flux which is defined as the deviation from the average of the total flight track. Simulated fluxes have been interpolated from model grid to exact location and time of flight overpass. The early flight moves from NE to SW, the return flight from SW to NE. So in the scatter plot the left side is the NE the middle the SW and the right side NE again.

BGD

5, 4161–4207, 2008

Simulation of carbon exchange using a regional model

H. W. Ter Maat and R. W. A. Hutjes

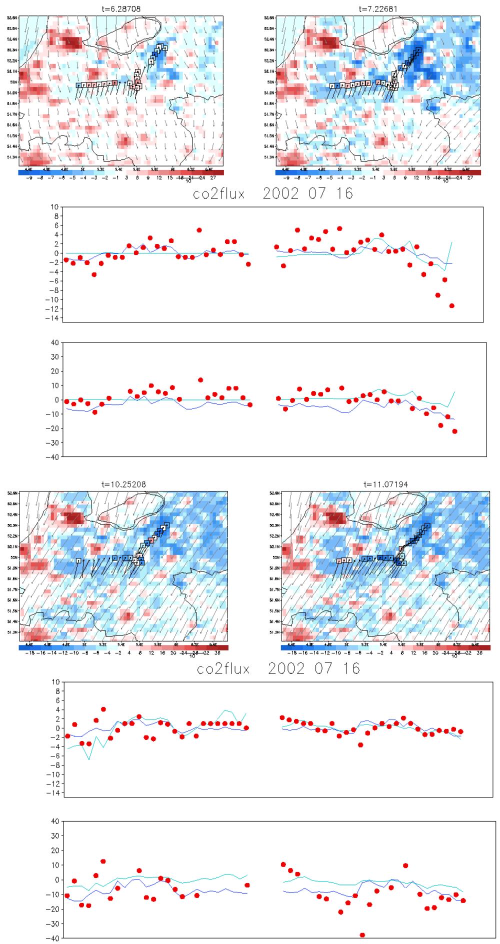

Fig. 11. Spatial comparison of carbon fluxes (μmol m^{-2} s^{-1}) against aircraft observations, for the flights on 16 July 2002 (top: 06:28 UTC, 07:22 UTC; bottom: 10:25 UTC, 11:07 UTC). Explanation of the maps is given in the caption accompanying Fig. 10.

BGD
5, 4161–4207, 2008

Simulation of carbon exchange using a regional model

H. W. Ter Maat and R. W. A. Hutjes

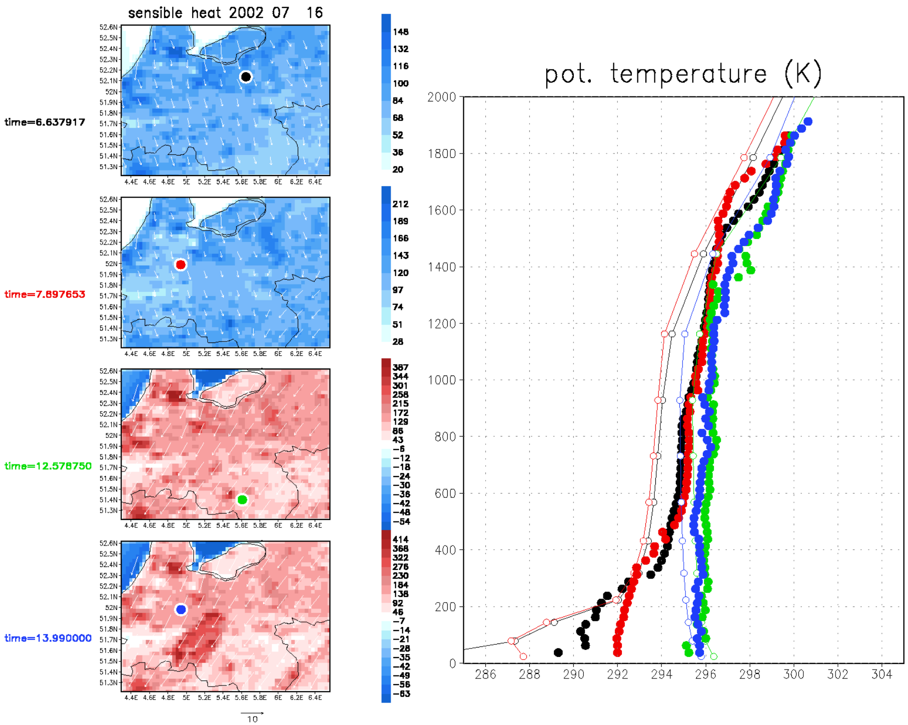

Fig. 12. Comparison of simulated profiles of potential temperature (K) against aircraft observations. Left panel: simulated surface sensible heat flux field at time of profile flight, with profile flight locations (coloured dots). Right panel: observed profiles (filled dots) and simulated profiles (open circles and lines). Note that the time sequence is black, red, green and blue.

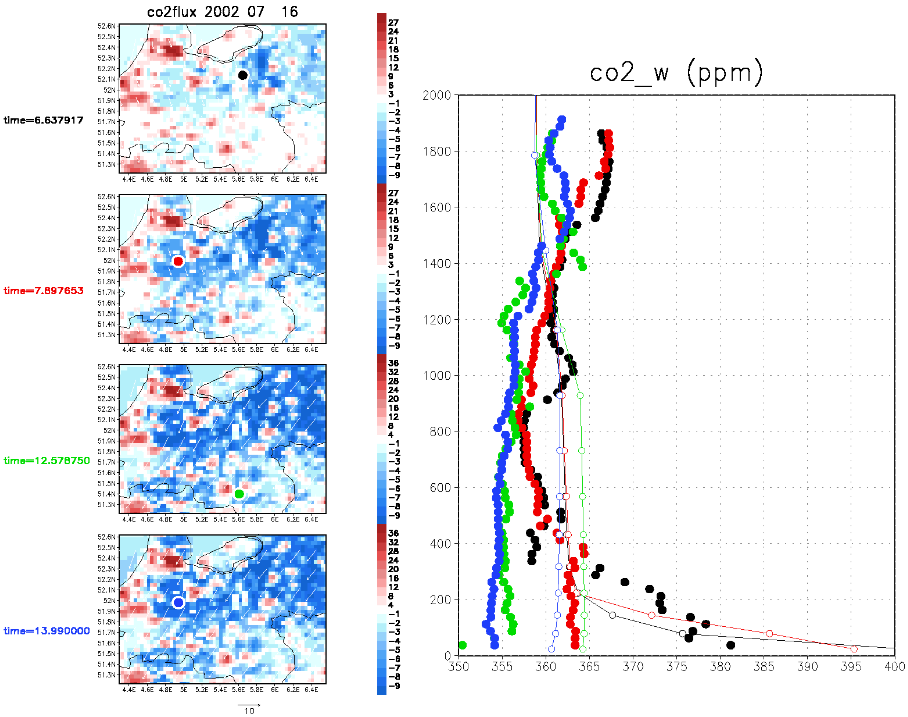

Fig. 13. Comparison of simulated profiles of CO_2 concentration (ppm) against aircraft observations. Left panel: simulated surface flux field at time of profile flight, with profile flight locations (coloured dots). Right panel: observed profiles (filled dots) and simulated profiles (open circles and lines). Note that the time sequence is black, red, green and blue.

BGD

5, 4161–4207, 2008

Title Page
Abstract Introduction
Conclusions References
Tables Figures
◀| |▶
◀ ▶
Back Close
Full Screen / Esc
Printer-friendly Version
Interactive Discussion

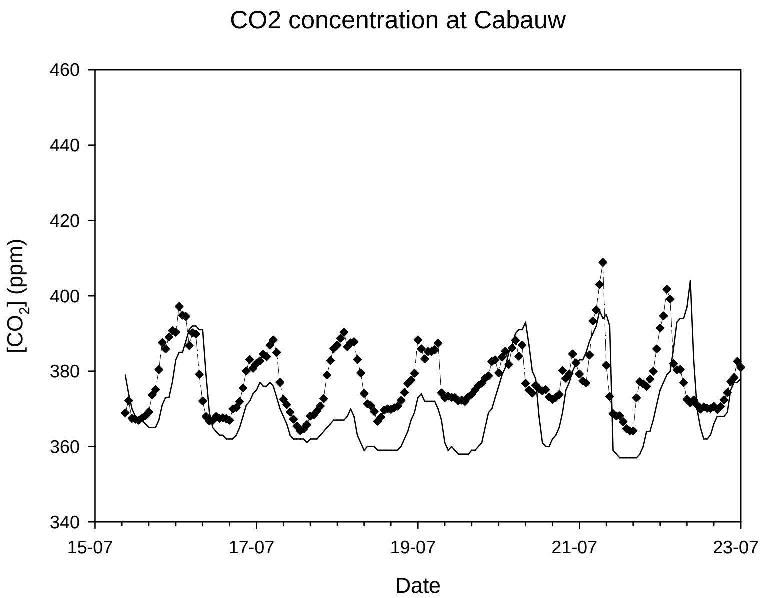

Fig. 14. Comparison of observed and simulated CO_2 concentration (ppm) at 60 m for Cabauw. Diamonds and dotted lines: observed values; orange lines simulated at a gridpoint nearest to the observational site representing the appropriate tile.

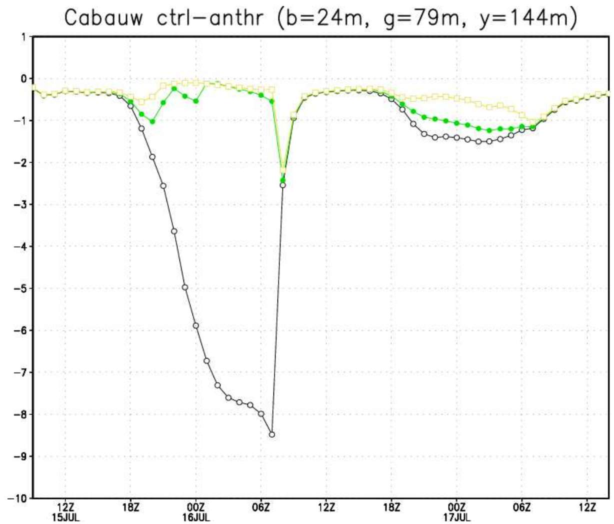

Fig. 15. Difference in simulated CO_2 concentration (ppm) at Cabauw between the control simulation and the simulation with an increase of 20% in anthropogenic emissions for three heights: Black: 24 m, green: 79 m, yellow: 144 m.

BGD
5, 4161–4207, 2008

H. W. Ter Maat and R. W. A. Hutjes

Title Page
Abstract | Introduction
Conclusions | References
Tables | Figures
◀◀ | ▶▶
◀ | ▶
Back | Close
Full Screen / Esc
Printer-friendly Version
Interactive Discussion

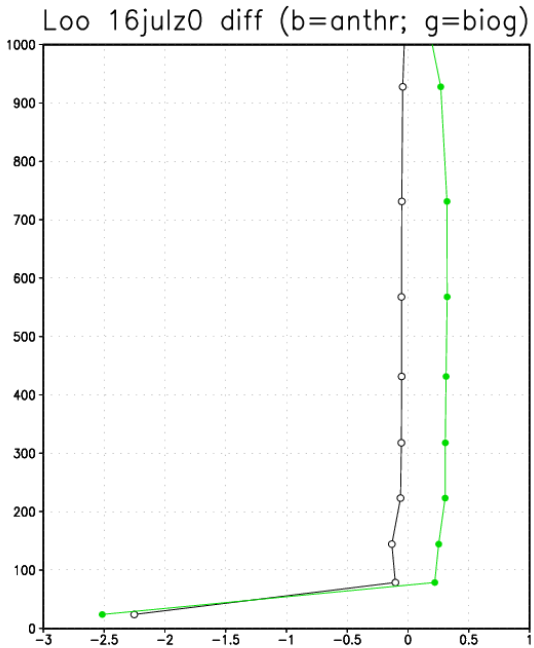

Fig. 16. Vertical profile at Loobos of the difference in simulated CO_2 concentration (ppm) between control simulation and anthropogenic simulation (black) and between control simulation and biogene simulation (green).

BGD

5, 4161–4207, 2008

Simulation of carbon exchange using a regional model

H. W. Ter Maat and R. W. A. Hutjes

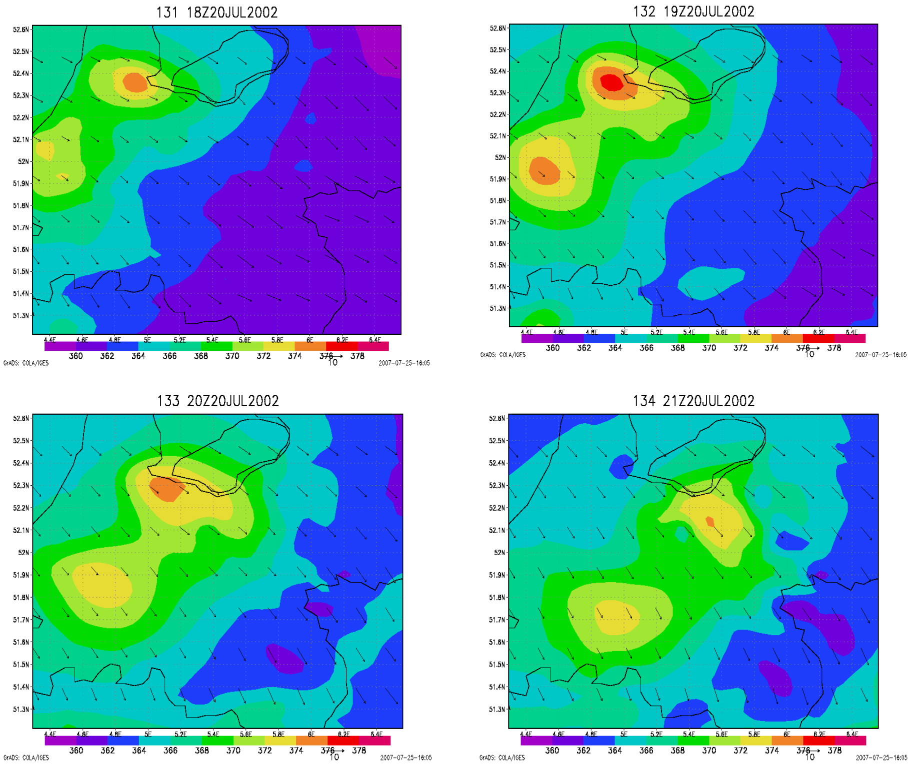

Fig. 17. CO_2 concentration snapshots (ppm) at lowest model level for 4 different times level at 20 July 2002 (left–right: 18:00 GMT–21:00 GMT with one hour steps).

BGD

5, 4161–4207, 2008

Simulation of carbon exchange using a regional model

H. W. Ter Maat and R. W. A. Hutjes